

Distribution of steel fibres in rectangular sections

David Dupont ^{a,*}, Lucie Vandewalle ^b

^a *Ergon NV, Marnixdreef 5, 2500 Lier, Belgium*

^b *Departement Burgerlijke Bouwkunde, Katholieke Universiteit Leuven, Kasteelpark Arenberg 40, 3001 Heverlee, Belgium*

Received 20 January 2003; accepted 22 March 2004

Abstract

In this paper a calculation method is explained to predict the total number of fibres crossing a rectangular section. The largest part of the paper deals with the theoretical calculation of an orientation factor. The orientation factor is defined here as the average length of the projection on the longitudinal axis of all fibres crossing a section, divided by the fibre length. Once the orientation factor is found, a simple calculation gives the number of fibres crossing a crack. Since the proposed approach is to a large extent new, there is a need for verification with test results. For this reason a fibre counting was done on 107 Rilem beam specimens, involving different fibre types. The comparison with the calculated number of fibres shows that the model provides good predictions of the number of fibres crossing a section.

© 2004 Elsevier Ltd. All rights reserved.

Keywords: Fibre distribution; Steel fibre concrete; Fibre orientation

1. Introduction

One of the most important properties of steel fibre concrete is its ability to transfer stresses across a cracked section. This ability is mostly translated into a toughness parameter [1], which is a measure for the energy consumed during a bending test. Experimental research at the Department of Civil Engineering of the K.U. Leuven and also elsewhere [2] has shown that there is a high degree of proportionality between the toughness and the number of effective fibres that are counted in the cracked section. A fibre was considered to be effective if the hook of the fibre was straightened after the two beam halves were separated. This conclusion creates an interest in knowing the number of effective fibres that cross a cracked section. The number of effective fibres is not only dependent on the fibre dosage, but also on the ori-

entation factor and the length efficiency factor [3,4]. In this paper only the total number of fibres (effective as well as non-effective) is determined. For further calculations it could be assumed that the number of effective fibres is proportional to the number of total fibres. The calculation of this coefficient of proportionality, which is dependent on the efficiency of the fibre, is not considered in this paper.

2. General approach

To calculate the total number of fibres, it is essential to know the orientation factor. It has been shown by Krenchel [5] that the number of fibres can be found as follows:

$$n = \alpha \frac{V_f}{A_f}$$

where n = number of fibres per unit surface; α = orientation coefficient; V_f = fibre volume fraction; A_f = cross-section of a fibre.

* Corresponding author. Tel.: +32 34 90 04 27; fax: +32 34 89 23 27.
E-mail address: David.dupont@ergon.be (D. Dupont).

The calculation of the orientation factor α has been the interest of many researchers [2–10]. First the orientation factor is calculated for the case the fibre can rotate freely in all directions. This is the case for a fibre in bulk (zone 1 in Fig. 1). Secondly one boundary condition is considered, parallel to the direction in which the orientation factor is determined. This simulates the proximity of one mould side (zone 2 in Fig. 1). And finally a second boundary condition is added, also parallel to the direction in which the orientation factor is determined, but now perpendicular to the first boundary condition. This simulates a fibre situated in a corner of the mould (zone 3 in Fig. 1).

b and h (see Fig. 1) are the width and the height of the beam section, while l_f stands for the fibre length. The following seven assumptions are made for calculating the orientation factor in each of these three areas:

- 1) The fibres are straight. For hooked end fibres the same orientation factor can be taken since the effect of the hooks is negligible on the orientation factor.
- 2) If the fresh concrete is vibrated for a long time or when it has a high workability (e.g. self compacting concrete), the fibres tend to orient in a horizontal plane [11]. This orientation effect depends highly on the vibration time and frequency and the workability and composition of the concrete and it is therefore very difficult to quantify. However, from other research [12] it is concluded that the vibration does not have a significant effect on the orientation if the specimen is only vibrated for 1 or 2 min and if

the workability of the fresh concrete is not too high. The effect of vibration on the orientation of the fibres is not considered here.

- 3) The location of the fibre in the beam is characterised by its point of gravity. Each point of the cross-section is considered to have an equal probability of being the gravity point of a fibre. Some researchers have found that there is an under reinforcement in the zones near to the boundaries while others have found the opposite. Here no preference is made [2,7].
- 4) The fibre orientation in area 1 (Fig. 1) is not influenced at all by the boundary conditions.
- 5) The fibre orientation in area 2 (Fig. 1) is only influenced by one side of the mould.
- 6) The fibre orientation in area 3 (Fig. 1) is influenced by two sides of the mould.
- 7) The top surface of the section is assumed to have the same boundary condition as the sides of the mould. After casting, this surface is smoothened so that there are no fibres sticking out. There could be a higher number of fibres at the surface due to the topping off and levelling of the specimen. This effect is not considered in this paper.

When the orientation factor for the areas 1, 2 and 3 (Fig. 1) are known to be α_1 , α_2 and α_3 , respectively, then the overall orientation factor can be calculated as follows by taking the geometrical average over the section:

$$\alpha = \frac{[\alpha_1 \times (b - l_f)(h - l_f) + \alpha_2 \times ((b - l_f)l_f + (h - l_f)l_f) + \alpha_3 \times l_f^2]}{bh} \quad (1)$$

with α_1 = orientation factor in zone 1 (Fig. 1); α_2 = orientation factor in zone 2 (Fig. 1); α_3 = orientation factor in zone 3 (Fig. 1).

3. Orientation factor in bulk

A fibre in bulk (zone 1 in Fig. 1) is not limited by any boundary condition and can rotate freely round its gravity point. If all the possible orientations of the fibre are considered, the end points of the fibre describe the surface of a sphere. Each point on the sphere has an equal probability to be the end of the fibre. This means that the probability that the fibre makes an angle θ with the longitudinal axis of the beam is proportional to the area dA (Fig. 2) with:

$$dA = \underbrace{\frac{\pi l_f^2}{2}}_{A1} \sin \theta \, d\theta \quad (2)$$

The contribution of the area dA to the orientation factor is then $\cos \theta dA$. Integrating this over half the sphere and dividing by the surface of half the sphere gives:

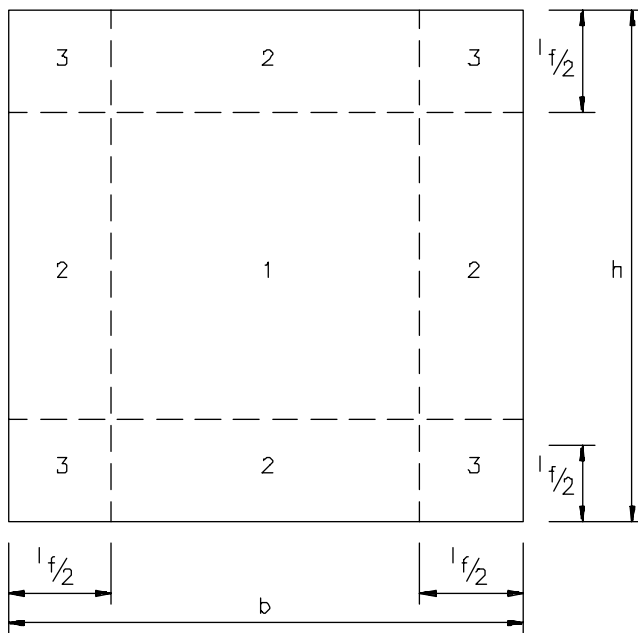


Fig. 1. Cross-section of a beam divided into three different orientation zones.

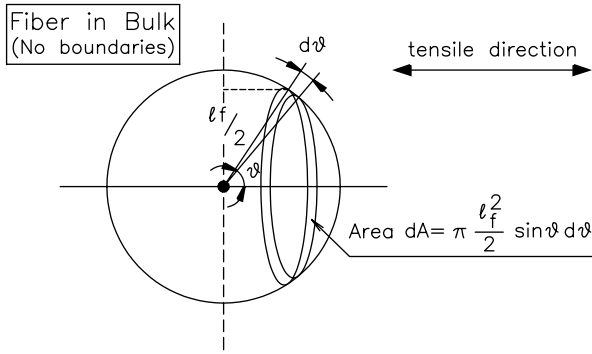


Fig. 2. A fibre in bulk.

$$\alpha_1 = \frac{\int_0^{\pi/2} \cos \theta dA}{2\pi \left(\frac{l_f}{2}\right)^2} = \frac{\int_0^{\pi/2} A1 \times \cos \theta d\theta}{2\pi \left(\frac{l_f}{2}\right)^2} = 0.5 \quad (3)$$

Based on stereological principles, Stroeven and Shah [8] come to the same result. The scenario depicted in Fig. 2 represents a situation when the embedment length is equal to half the fibre length. Li et al. [9] have also investigated the more common case in which the embedment length is different from half of the fibre length. This approach can be very interesting if it is the aim to calculate the pullout response of the fibre, since for each possible embedment length, the possible orientations can be found. In this paper it was only the aim to propose a simple method to calculate the average orientation coefficient of the fibres, without considering the possible embedment lengths of the fibres.

4. Orientation factor of a fibre with 1 boundary condition

This is the case in area 2 in Fig. 1. Suppose that the gravity point of the fibre is within a distance y from the mould with $y < l_f/2$. The fibre can no longer rotate freely. The end points describe a sphere that is cut on

one side by a sphere cap (Fig. 3). If θ is again the angle of the fibre with the longitudinal axis and θ increases from 0, there is no problem as long as

$$\theta < \theta_{\text{crit}} = \arcsin\left(\frac{2y}{l_f}\right) \quad (4)$$

Under this condition the elementary surface dA is still given by Eq. (2). When the angle θ is bigger than θ_{crit} , the area dA reduces to the bold lines in the cut A–A (Fig. 3).

$$dA = \underbrace{l_f^2 \sin \theta}_{A2} \cdot \arcsin\left(\frac{2y}{l_f \sin \theta}\right) d\theta \quad (5)$$

For a fibre with its gravity point at a distance y from the side of the mould, the orientation coefficient becomes:

$$\alpha_y = \frac{\int_0^{\arcsin\left(\frac{2y}{l_f}\right)} A1 \times \cos \theta d\theta + \int_{\arcsin\left(\frac{2y}{l_f}\right)}^{\pi/2} A2 \times \cos \theta d\theta}{2\pi \left(\frac{l_f}{2}\right)^2 - 2\pi \frac{l_f}{2} \left(\frac{l_f}{2} - y\right)} \quad (6)$$

This means that the average orientation coefficient for area 2 is

$$\alpha_2 = \frac{2}{l_f} \int_0^{l_f/2} \left[\frac{\int_0^{\arcsin\left(\frac{2y}{l_f}\right)} A1 \times \cos \theta d\theta + \int_{\arcsin\left(\frac{2y}{l_f}\right)}^{\pi/2} A2 \times \cos \theta d\theta}{2\pi \left(\frac{l_f}{2}\right)^2 - 2\pi \frac{l_f}{2} \left(\frac{l_f}{2} - y\right)} \right] dy \quad (7)$$

In the expression for α_2 , l_f should be seen as a parameter. Numerical integration of expression (7) returns for α_2 the value 0.60, which is independent of the fibre length. Although the fibre length is one of the parameters in expression (7), it has no influence on the result of the expression. The fibre length only makes a difference in the overall orientation coefficient, which is calculated in formula (1).

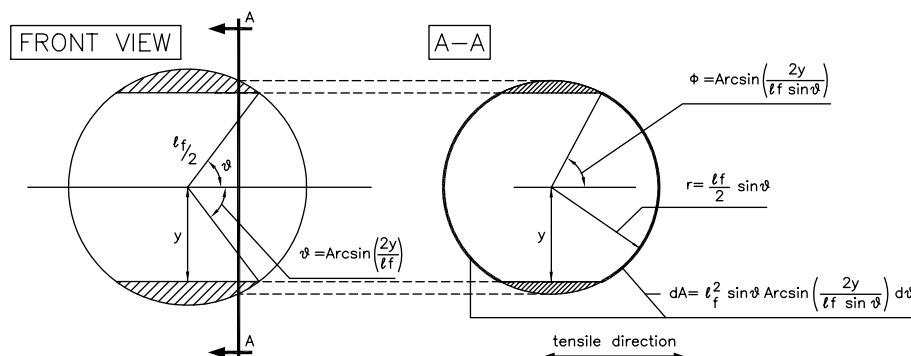


Fig. 3. A fibre near one side of the mould.

5. Orientation factor of a fibre with 2 boundary conditions

This is the case for area 3 in Fig. 1. Consider a fibre with gravity centre at a distance y from one mould-side and at a distance z from another mouldside that is perpendicular to the first (Fig. 4). There are two cases:

5.1. $y < z < l_f/2$

There is no problem as long as

$$\theta < \theta_{\text{crit}} = \arcsin\left(\frac{2y}{l_f}\right) \quad (8)$$

When:

$$\theta_{\text{crit}} = \arcsin\left(\frac{2y}{l_f}\right) \leq \theta \leq \theta_{\text{crit}2} = \arcsin\left(\frac{2z}{l_f}\right) \quad (9)$$

the area dA can be found with Eq. (5).

If $\theta > \theta_{\text{crit}2}$, it can be concluded from Fig. 4 that the area dA is

$$dA = \underbrace{l_f^2 \sin \theta \left[\arcsin\left(\frac{2y}{l_f \sin \theta}\right) - \arccos\left(\frac{2z}{l_f \sin \theta}\right) \right]}_{A_3} d\theta \quad (10)$$

Eq. (10) is only valid provided that:

$$z^2 + y^2 > \left(\frac{l_f}{2} \sin \theta\right)^2 \quad (11)$$

If Eq. (11) is not true, dA should be set equal to 0. The total area of the sphere that is cut on four sides by a spherecap is calculated as follows:

$$S_1 = \int_0^{\arcsin\left(\frac{2y}{l_f}\right)} A_1 d\theta + \int_{\arcsin\left(\frac{2y}{l_f}\right)}^{\arcsin\left(\frac{2z}{l_f}\right)} A_2 d\theta + \int_{\arcsin\left(\frac{2z}{l_f}\right)}^{\pi/2} \text{Max}[0; A_3] d\theta \quad (12)$$

5.2. $z < y < l_f/2$

For $\theta < \theta_{\text{crit}2} = \arcsin\left(\frac{2z}{l_f}\right)$ the surface dA is given by Eq. (2). For $\theta_{\text{crit}2} < \theta < \theta_{\text{crit}}$ the surface dA should be calculated as

$$dA = \underbrace{l_f^2 \sin \theta \times \arcsin\left(\frac{2z}{l_f \sin \theta}\right)}_{A_4} d\theta \quad (13)$$

Eq. (13) is simply found by replacing y for z in Eq. (5). For $\theta > \theta_{\text{crit}}$ the area dA is again calculated by means of Eq. (10) taking into consideration the restriction of Eq. (11). The total area of the sphere that is cut on four sides by a spherecap is calculated as follows:

$$S_2 = \int_0^{\arcsin\left(\frac{2z}{l_f}\right)} A_1 d\theta + \int_{\arcsin\left(\frac{2z}{l_f}\right)}^{\arcsin\left(\frac{2y}{l_f}\right)} A_4 d\theta + \int_{\arcsin\left(\frac{2y}{l_f}\right)}^{\pi/2} \text{Max}[0; A_3] d\theta \quad (14)$$

Bringing everything together an expression can be formulated for the orientation coefficient α_3 (Eq. (15)).

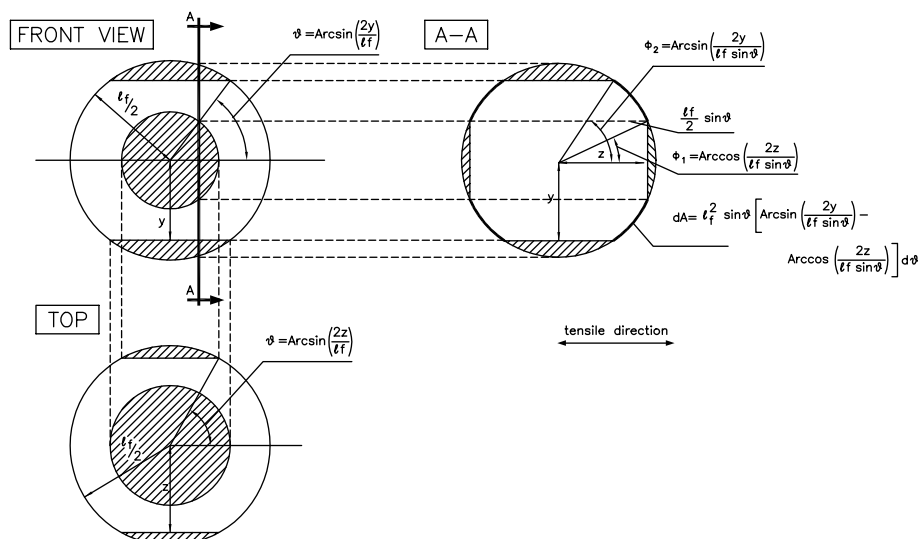


Fig. 4. A fibre in a corner of the mould.

$$\alpha_3 = \frac{4}{l_f^2} \int_0^{l_f/2} \left[\int_0^y \frac{\int_0^{\arcsin(\frac{2y}{l_f})} A_1 \cos \theta d\theta + \int_{\arcsin(\frac{2y}{l_f})}^{\arcsin(\frac{2y}{l_f})} A_4 \cos \theta d\theta + \int_{\arcsin(\frac{2y}{l_f})}^{\pi/2} \text{Max}[0; A_3] \cos \theta d\theta}{S_2} dz + \int_y^{l_f/2} \frac{\int_0^{\arcsin(\frac{2y}{l_f})} A_1 \cos \theta d\theta + \int_{\arcsin(\frac{2y}{l_f})}^{\arcsin(\frac{2y}{l_f})} A_2 \cos \theta d\theta + \int_{\arcsin(\frac{2y}{l_f})}^{\pi/2} \text{Max}[0; A_3] \cos \theta d\theta}{S_1} dz \right] dy \quad (15)$$

Numerical integration of this integral converges slowly into the value 0.84. This value is independent on l_f .

6. Calculation example

At the Department of Civil Engineering of the K.U. Leuven a series of beams with cross-section 150 mm × 150 mm were tested. Before testing the beam was notched with a notch of 25 mm. After testing the beam was broken in two halves and the fibres were counted in the remaining ligament section (Fig. 5).

Two new areas can be seen (areas 4 and 5). To obtain the average orientation coefficient for these areas, a simple modification of Eqs. (7) and (15) satisfies. It is enough to let the integration for y start from the notch depth instead of from 0 and then of course also not divide by $l_f/2$ but by $(l_f/2 - \text{notch depth})$. Implementing this, results in Eqs. (16) and (17).

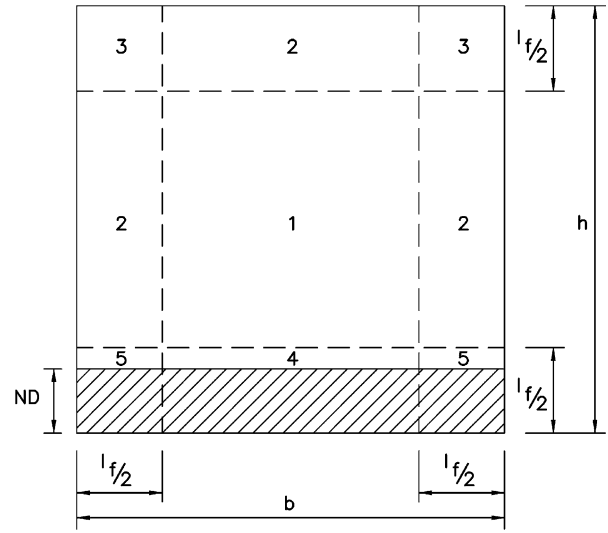


Fig. 5. Notched cross-section.

$$\alpha_4 = \frac{1}{(l_f/2 - ND)} \int_{ND}^{l_f/2} \left[\frac{\int_0^{\arcsin(\frac{2y}{l_f})} A1 \times \cos \theta d\theta + \int_{\arcsin(\frac{2y}{l_f})}^{\pi/2} A2 \times \cos \theta d\theta}{2\pi(\frac{l_f}{2})^2 - 2\pi\frac{l_f}{2}(\frac{l_f}{2} - y)} \right] dy \quad (16)$$

For the example considered here this results in: $\alpha_4 = 0.53$

$$\alpha_5 = \frac{\int_{ND}^{l_f/2} \left[\int_0^y \frac{\int_0^{\arcsin(\frac{2y}{l_f})} A_1 \cos \theta d\theta + \int_{\arcsin(\frac{2y}{l_f})}^{\arcsin(\frac{2y}{l_f})} A_4 \cos \theta d\theta + \int_{\arcsin(\frac{2y}{l_f})}^{\pi/2} \text{Max}[0; A_3] \cos \theta d\theta}{S_2} dz + \int_y^{l_f/2} \frac{\int_0^{\arcsin(\frac{2y}{l_f})} A_1 \cos \theta d\theta + \int_{\arcsin(\frac{2y}{l_f})}^{\arcsin(\frac{2y}{l_f})} A_2 \cos \theta d\theta + \int_{\arcsin(\frac{2y}{l_f})}^{\pi/2} \text{Max}[0; A_3] \cos \theta d\theta}{S_1} dz \right] dy}{((l_f/2) \times (l_f/2 - ND))} \quad (17)$$

Table 1
Comparison of the experimental and theoretical number of fibres

No. (#)	Fiber dosage (kg/m ³)	Fiber type	l_f (mm)	d_f (mm)	α_4	α_5	α	exp. (#)	calc. (#)	Ratio calc./exp.
1	20	RC 65/60 BN	60	0.92	0.53	0.69	0.58	92	41	0.45
2	20	RC 65/60 BN	60	0.92	0.53	0.69	0.58	68	41	0.61
3	20	RC 65/60 BN	60	0.92	0.53	0.69	0.58	77	41	0.54
4	20	RC 65/60 BN	60	0.92	0.53	0.69	0.58	74	41	0.56
5	20	RC 65/60 BN	60	0.92	0.53	0.69	0.58	127	41	0.32
6	20	RC 65/60 BN	60	0.92	0.53	0.69	0.58	38	41	1.09
7	20	RC 65/60 BN	60	0.92	0.53	0.69	0.58	66	41	0.63
8	20	RC 65/60 BN	60	0.92	0.53	0.69	0.58	55	41	0.75
9	20	RC 65/60 BN	60	0.92	0.53	0.69	0.58	84	41	0.49
10	20	RC 65/60 BN	60	0.92	0.53	0.69	0.58	44	41	0.94
11	20	RC 65/60 BN	60	0.92	0.53	0.69	0.58	57	41	0.72
12	20	RC 65/60 BN	60	0.92	0.53	0.69	0.58	30	41	1.38
13	20	RC 65/60 BN	60	0.92	0.53	0.69	0.58	50	41	0.83
14	20	RC 65/60 BN	60	0.92	0.53	0.69	0.58	35	41	1.18
15	20	RC 65/60 BN	60	0.92	0.53	0.69	0.58	48	41	0.86
16	20	RC 65/60 BN	60	0.92	0.53	0.69	0.58	45	41	0.92
17	20	RC 65/60 BN	60	0.92	0.53	0.69	0.58	36	41	1.15
18	60	RC 65/60 BN	60	0.92	0.53	0.69	0.58	224	124	0.55
19	60	RC 65/60 BN	60	0.92	0.53	0.69	0.58	324	124	0.38
20	60	RC 65/60 BN	60	0.92	0.53	0.69	0.58	326	124	0.38
21	60	RC 65/60 BN	60	0.92	0.53	0.69	0.58	246	124	0.50
22	60	RC 65/60 BN	60	0.92	0.53	0.69	0.58	237	124	0.52
23	60	RC 65/60 BN	60	0.92	0.53	0.69	0.58	294	124	0.42
24	60	RC 65/60 BN	60	0.92	0.53	0.69	0.58	222	124	0.56
25	60	RC 65/60 BN	60	0.92	0.53	0.69	0.58	159	124	0.78
26	60	RC 65/60 BN	60	0.92	0.53	0.69	0.58	183	124	0.68
27	60	RC 65/60 BN	60	0.92	0.53	0.69	0.58	237	124	0.52
28	60	RC 65/60 BN	60	0.92	0.53	0.69	0.58	171	124	0.72
29	60	RC 65/60 BN	60	0.92	0.53	0.69	0.58	270	124	0.46
30	60	RC 65/60 BN	60	0.92	0.53	0.69	0.58	175	124	0.71
31	60	RC 65/60 BN	60	0.92	0.53	0.69	0.58	110	124	1.13
32	60	RC 65/60 BN	60	0.92	0.53	0.69	0.58	159	124	0.78
33	60	RC 65/60 BN	60	0.92	0.53	0.69	0.58	166	124	0.75
34	60	RC 65/60 BN	60	0.92	0.53	0.69	0.58	179	124	0.69
35	60	RC 65/60 BN	60	0.92	0.53	0.69	0.58	175	124	0.71
36	40	RC 65/60 BN	60	0.92	0.53	0.69	0.58	72	83	1.15
37	40	RC 65/60 BN	60	0.92	0.53	0.69	0.58	94	83	0.88
38	40	RC 65/60 BN	60	0.92	0.53	0.69	0.58	91	83	0.91
39	40	RC 65/60 BN	60	0.92	0.53	0.69	0.58	70	83	1.18
40	40	RC 65/60 BN	60	0.92	0.53	0.69	0.58	81	83	1.02
41	40	RC 65/60 BN	60	0.92	0.53	0.69	0.58	43	83	1.92
42	40	RC 65/60 BN	60	0.92	0.53	0.69	0.58	85	83	0.97
43	40	RC 65/60 BN	60	0.92	0.53	0.69	0.58	79	83	1.04
44	40	RC 65/60 BN	60	0.92	0.53	0.69	0.58	72	83	1.15
45	40	RC 65/60 BN	60	0.92	0.53	0.69	0.58	73	83	1.13
46	40	RC 65/60 BN	60	0.92	0.53	0.69	0.58	67	83	1.23
47	40	RC 80/35 BN	35	0.44			0.54	264	344	1.30
48	40	RC 80/35 BN	35	0.44			0.54	249	344	1.38
49	40	RC 80/35 BN	35	0.44			0.54	250	344	1.37
50	40	RC 80/35 BN	35	0.44			0.54	273	344	1.26
51	40	RC 80/35 BN	35	0.44			0.54	304	344	1.13
52	40	RC 80/35 BN	35	0.44			0.54	294	344	1.17
53	60	RC 80/35 BN	35	0.44			0.54	382	516	1.35
54	60	RC 80/35 BN	35	0.44			0.54	329	516	1.57
55	60	RC 80/35 BN	35	0.44			0.54	278	516	1.85
56	60	RC 80/35 BN	35	0.44			0.54	375	516	1.37
57	60	RC 80/35 BN	35	0.44			0.54	314	516	1.64
58	60	RC 80/35 BN	35	0.44			0.54	327	516	1.58
59	50	RC 80/60 BN	60	0.75	0.53	0.69	0.58	145	156	1.08
60	50	RC 80/60 BN	60	0.75	0.53	0.69	0.58	144	156	1.09
61	50	RC 80/60 BN	60	0.75	0.53	0.69	0.58	189	156	0.83
62	50	RC 80/60 BN	60	0.75	0.53	0.69	0.58	200	156	0.78

Table 1 (continued)

No. (#)	Fiber dosage (kg/m ³)	Fiber type	l_f (mm)	d_f (mm)	α_4	α_5	α	exp. (#)	calc. (#)	Ratio calc./exp.
63	50	RC 80/60 BN	60	0.75	0.53	0.69	0.58	107	156	1.46
64	50	RC 80/60 BN	60	0.75	0.53	0.69	0.58	185	156	0.84
65	50	RC 80/60 BN	60	0.75	0.53	0.69	0.58	135	156	1.16
66	50	RC 80/60 BN	60	0.75	0.53	0.69	0.58	158	156	0.99
67	25	RC 65/60 BN	60	0.92	0.53	0.69	0.58	19	52	2.71
68	25	RC 65/60 BN	60	0.92	0.53	0.69	0.58	47	52	1.10
69	25	RC 80/60 BP	60	0.75	0.53	0.69	0.58	84	78	0.93
70	25	RC 65/60 BN	60	0.92	0.53	0.69	0.58	40	52	1.29
71	75	RC 65/60 BN	60	0.92	0.53	0.69	0.58	184	155	0.84
72	75	RC 65/60 BN	60	0.92	0.53	0.69	0.58	171	155	0.90
73	75	RC 65/60 BN	60	0.92	0.53	0.69	0.58	138	155	1.12
74	25	RC 80/60 BP	60	0.75	0.53	0.69	0.58	89	78	0.88
75	25	RC 80/60 BP	60	0.75	0.53	0.69	0.58	96	78	0.81
76	25	RC 80/60 BP	60	0.75	0.53	0.69	0.58	79	78	0.99
77	25	RC 80/60 BP	60	0.75	0.53	0.69	0.58	83	78	0.94
78	25	RC 80/60 BP	60	0.75	0.53	0.69	0.58	67	78	1.17
79	25	RC 80/60 BP	60	0.75	0.53	0.69	0.58	67	78	1.17
80	25	RC 80/60 BP	60	0.75	0.53	0.69	0.58	76	78	1.03
81	25	RC 80/60 BP	60	0.75	0.53	0.69	0.58	110	78	0.71
82	25	RC 80/60 BP	60	0.75	0.53	0.69	0.58	64	78	1.22
83	25	RC 65/60 BN	60	0.92	0.53	0.69	0.58	51	52	1.01
84	25	RC 65/60 BN	60	0.92	0.53	0.69	0.58	60	52	0.86
85	25	RC 65/60 BN	60	0.92	0.53	0.69	0.58	60	52	0.86
86	25	RC 65/60 BN	60	0.92	0.53	0.69	0.58	47	52	1.10
87	25	RC 65/60 BN	60	0.92	0.53	0.69	0.58	59	52	0.87
88	25	RC 65/60 BN	60	0.92	0.53	0.69	0.58	61	52	0.85
89	25	RC 65/60 BN	60	0.92	0.53	0.69	0.58	29	52	1.78
90	25	RC 65/60 BN	60	0.92	0.53	0.69	0.58	45	52	1.15
91	50	RC 80/60 BN	60	0.75	0.53	0.69	0.58	172	156	0.91
92	50	RC 80/60 BN	60	0.75	0.53	0.69	0.58	153	156	1.02
93	75	RC 65/60 BN	60	0.92	0.53	0.69	0.58	199	155	0.78
94	75	RC 65/60 BN	60	0.92	0.53	0.69	0.58	137	155	1.13
95	75	RC 65/60 BN	60	0.92	0.53	0.69	0.58	158	155	0.98
96	75	RC 65/60 BN	60	0.92	0.53	0.69	0.58	168	155	0.92
97	75	RC 65/60 BN	60	0.92	0.53	0.69	0.58	182	155	0.85
98	75	RC 65/60 BN	60	0.92	0.53	0.69	0.58	136	155	1.14
99	35	RC 65/40 BN	40	0.62			0.55	146	154	1.05
100	35	RC 65/40 BN	40	0.62			0.55	124	154	1.24
101	35	RC 65/40 BN	40	0.62			0.55	143	154	1.08
102	60	RC 65/40 BN	40	0.62			0.55	197	264	1.34
103	60	RC 65/40 BN	40	0.62			0.55	216	264	1.22
104	60	RC 65/40 BN	40	0.62			0.55	213	264	1.24
105	60	RC 65/60 BN	60	0.92	0.53	0.69	0.58	98	124	1.26
106	60	RC 65/60 BN	60	0.92	0.53	0.69	0.58	127	124	0.97
107	60	RC 65/60 BN	60	0.92	0.53	0.69	0.58	89	124	1.39
Average of all 107 beams										1.002
Coefficient of variation										36%

For the example considered here, this results in: $\alpha_5 = 0.69$. The value of α_4 and α_5 , unlike α_1 , α_2 and α_3 , are dependent on the fibre length and the notch depth. In this example a fibre length of 60mm was taken. In the test results also fibres with a length of 35mm and 40mm have been used. The calculation for this length is of course similar, but since the depth of the notch is

in these cases larger than half of the fibre length, there is no need for α_4 and α_5 .

By means of a simple integration program α_4 and α_5 can be calculated for each specific case. For normal applications the problem of a notch is not existing. The overall orientation coefficient can be calculated with the following formula:

$$\alpha = \frac{\alpha_1(b - l_f)(h - l_f) + \alpha_2[(b - l_f)l_f/2 + (h - l_f)l_f] + \alpha_3l_f^2/2 + (l_f/2 - ND)[\alpha_4(b - l_f) + \alpha_5l_f]}{b(h - ND)}$$

For a fibre length of 60 mm this results in $\alpha = 0.58$. In case the notch is deeper than $l_f/2$, the following formula should be used to calculate the overall orientation coefficient:

$$\alpha = \frac{\alpha_1(b - l_f)(h - l_f/2 - ND) + \alpha_2[(b - l_f)l_f/2 + (h - l_f/2 - ND)l_f] + \alpha_3l_f^2/2}{b(h - ND)}$$

An average number of fibres in a section can be calculated:

$$N = \frac{G \times \alpha}{\frac{\pi \times d_f^2}{4} \times \rho_s} \times b \times h$$

with N is the theoretical number of fibres in the cross-section [#]; G the amount of fibres in the concrete [kg/m³]; α the orientation coefficient; b the width of the beam section [mm]; h the height of the remaining ligament of the beam section [mm]; d_f the diameter of a fibre [mm]; ρ_s the density of the steel of the fibres [kg/m³].

This results in Table 1.

7. Conclusions

This paper describes a calculation procedure for calculating the total number of fibres crossing a rectangular beam section. Most of the paper is dedicated to finding an expression for the orientation coefficient of a certain combination of fibre type and cross-section. This was done taking into account boundary conditions in two opposite directions. The comparison between the calculated and the experimentally obtained total number of fibres shows that the overall agreement is acceptable. However, as expected, for some specimens the deviation from the average value is rather big. This large scatter can also be found in the results of the bending test and is considered to be inherent to the material. The largest advantage of the proposed method is that it is very simple to implement for any combination of fibre type and cross-section.

Acknowledgments

Part of this study was conducted in the framework of the Brite Euram project “Test and Design Methods for Steel Fibre Reinforced Concrete”, contract no. BRPR-CT98-0813. The partners in the project are: N.V. Bekaert S.A. (Belgium, coordinator), Centre Scientifique et

Technique de la Construction (Belgium), Katholieke Universiteit Leuven (Belgium), Technical University of Denmark (Denmark), Balfour Beatty Rail Ltd. (Great Britain), University of Wales Cardiff (Great Britain),

Fertig-Decken-Union GmbH (Germany), Ruhr-University-Bochum (Germany), Technical University of Braunschweig (Germany), FCC Construcción S.A. (Spain), Universitat Politècnica de Catalunya (Spain).

References

- [1] Rilem TC162-TDF, Test and design methods for steel fibre reinforced concrete: Bending test. *Mater Struct* 2000;33(March): 75–81.
- [2] Van Gysel A. Studie van het uittrekgedrag van staalvezels ingebed in een cementgebonden matrix met toepassing op staalvezelbeton onderworpen aan buiging. Doctoral thesis at University of Ghent (Belgium), 2000, p. IV99–VI2.
- [3] Stroeven P. Steel fibre reinforcement at boundaries in concrete elements. In: *Proceedings of the Third International Workshop on High Performance Fiber Reinforced Cement Composites (HPRCC3)*, Mainz (Germany), 16–19 May 1999, p. 413–21.
- [4] Stroeven P. Effectiveness of steel wire reinforcement in a boundary layer of concrete. *Acta Stereol* 1991;10/1:113–22.
- [5] Krenchel H. Fibre spacing and specific fibre surface. In: Neville A, editor. *Fibre reinforced cement and concrete*. UK: The Construction Press; 1975. p. 69–79.
- [6] Kooiman AG. Modelling steel fibre reinforced concrete for structural design. Doctoral Thesis at the Technical University of Delft (The Netherlands), 2000, p. 87–106.
- [7] Stroeven P. Local strength reduction at boundaries due to non-uniformity of steel fibre distribution. In: *Proceedings of the international conference “Specialist Techniques and Materials for Concrete Construction”*, Dundee (UK), 8–10 September 1999, p. 377–87.
- [8] Stroeven P, Shah SP. Use of radiography-image analysis for steel fibre reinforced concrete. In: Swamy RN, editor. *Testing and test methods of fibre cement composites*. UK: The Construction Press; 1978. p. 275–88.
- [9] Li VC, Wang Y, Backer S. A micromechanical model of tension-softening and bridging toughening of short random fiber reinforced brittle matrix composites. *J Mech Phys Solids* 1991; 39(no. 5):607–25.
- [10] Soroushian P, Lee C. Distribution and orientation of fibers in steel fiber reinforced concrete. *ACI Mater J* 1990;87(no. 5):433–9.
- [11] Grunewald S, Walraven JC. High strength self-compacting fibre reinforced concrete: behaviour in the fresh and hardened state. *FIB Conference Leipzig*, 2002.
- [12] Gettu R, Barragan Bryan B, Gardner Diane, Ferreira Luiz Eduardo T. Study of the distribution and orientation of fibres in cast cylinders. Internal report of universitat politècnica de Catalunya (Spain), 2000.